

## **Supplementary Information for**

**"Heterogeneous cooling subsidence of oceanic  
lithosphere controlled by spreading rate"**

by Irina M. Artemieva

This PDF file includes:

Supplementary Figure S1. Age of seafloor, thickness of sediments and subdivision of the global ocean into 9 domains and 94 segments.

Supplementary Figure S2. Examples illustrating the effect of sediment correction on bathymetry versus age evolution.

Supplementary Figure S3. Comparison of subsidence rate and zero-age bathymetry for 94 ocean segments (present study) with previous studies.

Supplementary Figure S4. Area-weighted average values for oceanic segments determined in the present study.

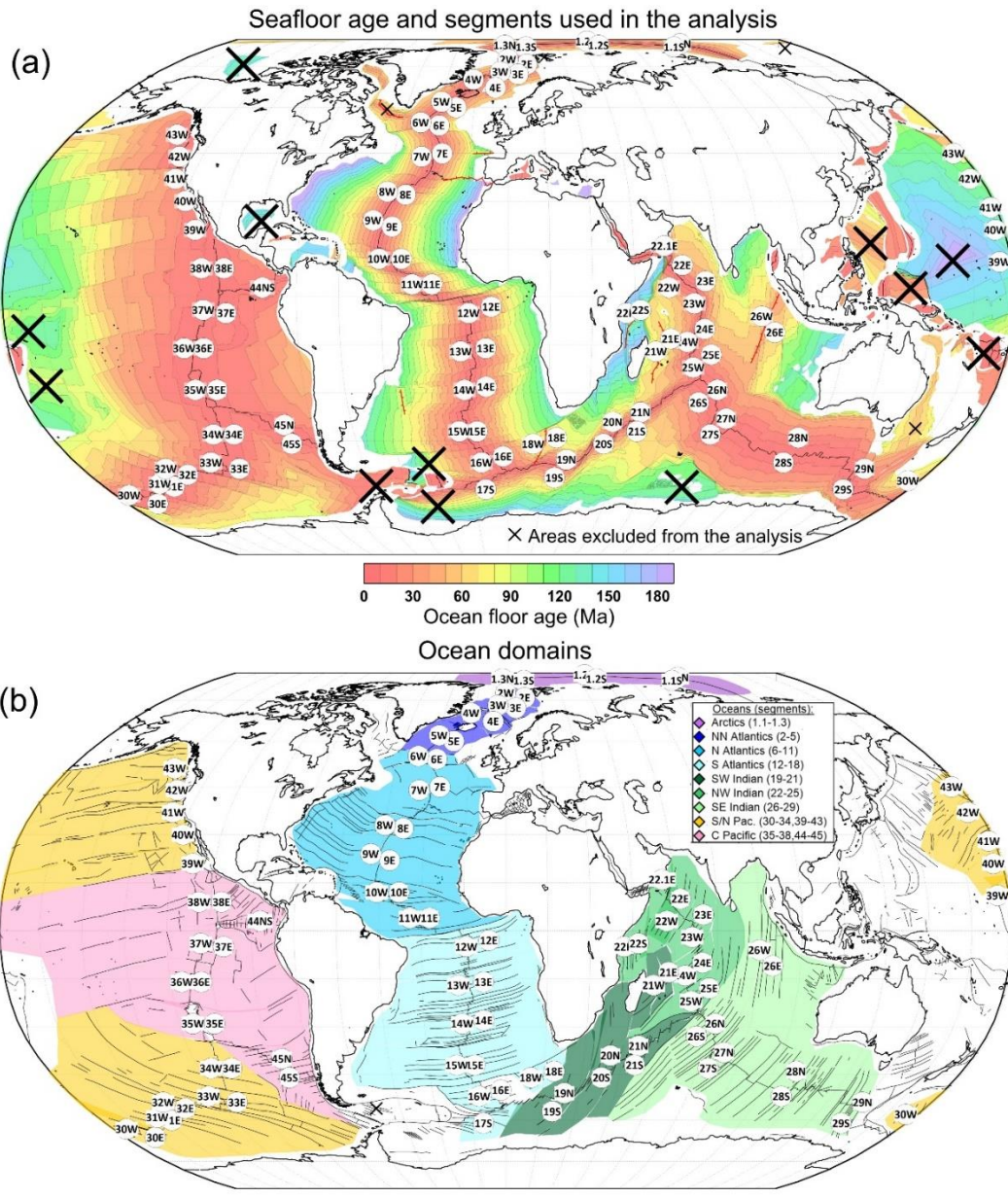
Supplementary Figure S5. Age distribution of anomalous oceans impacted by hotspots.

Supplementary Figure S6. Global correlations between ocean subsidence parameters.

Supplementary Table S1. Previous analyses of oceanic lithosphere subsidence with supplementary References.

References to Table S1.

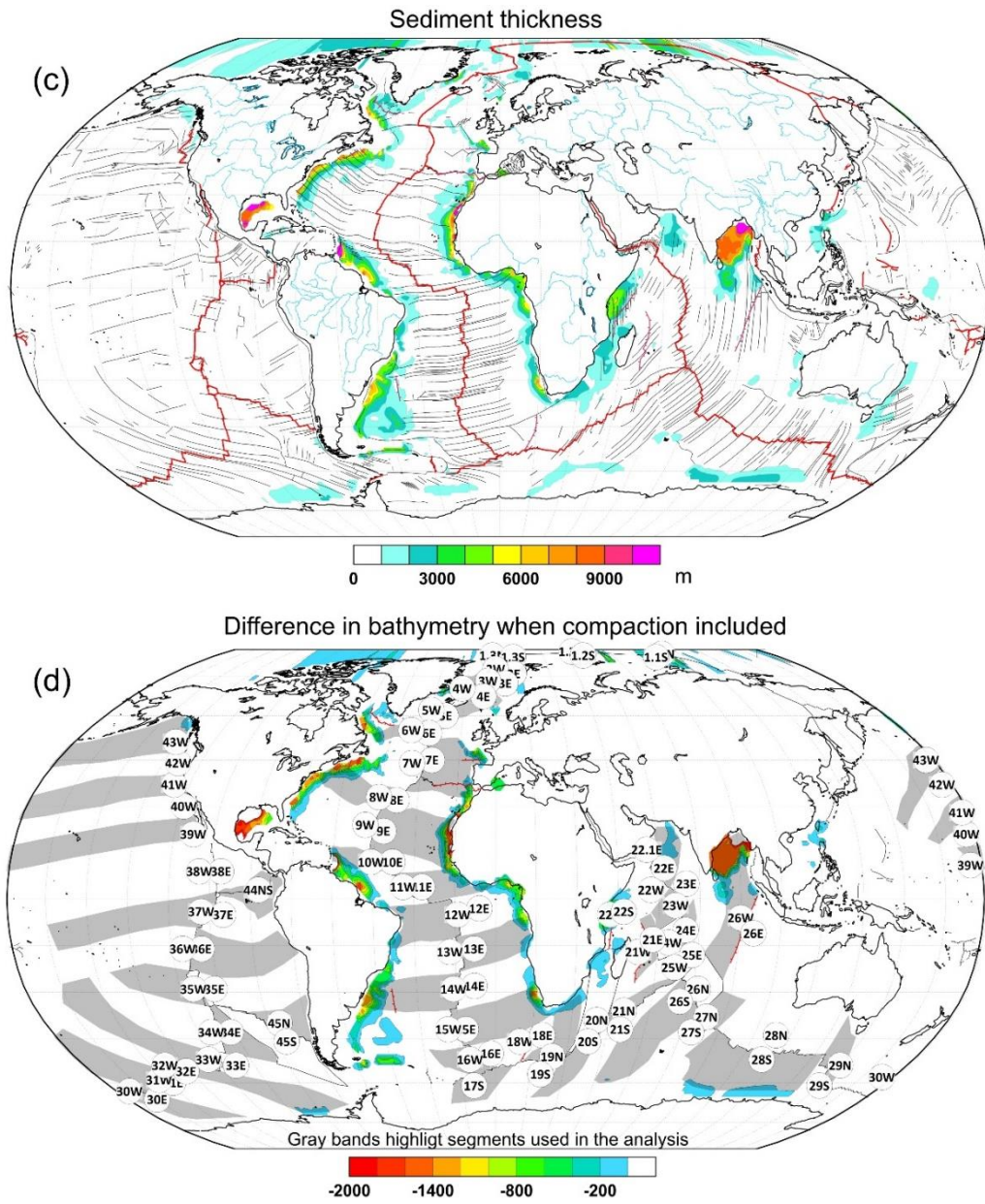
Supplementary Table S2. Parameters of bathymetry evolution calculated for 94 ocean segments



### Supplementary Figure S1.

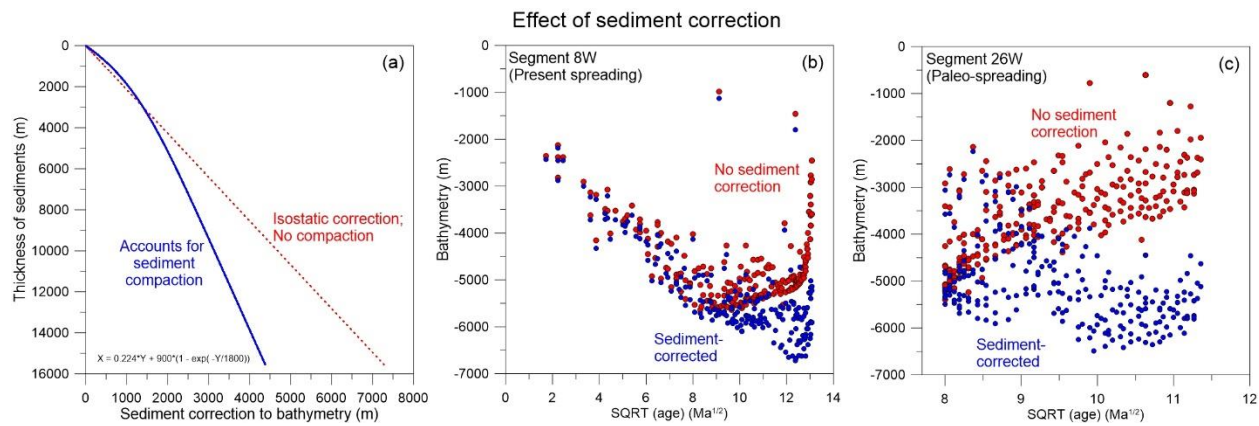
(a) Age of seafloor (*Seton et al., 2020*). Circles with numbers - 94 ocean segments used in the analysis, their coordinates and numbers are detailed in Table S2. Crosses mark areas that were excluded, e.g. due to their uncertain relation to spreading ridges (West Pacific). Red lines – paleo-spreadings.

(b) Subdivision of the global ocean to 9 color-coded ocean domains analyzed in the present study. Thin black lines – major transform faults.



### Supplementary Figure S1. Cont'd.

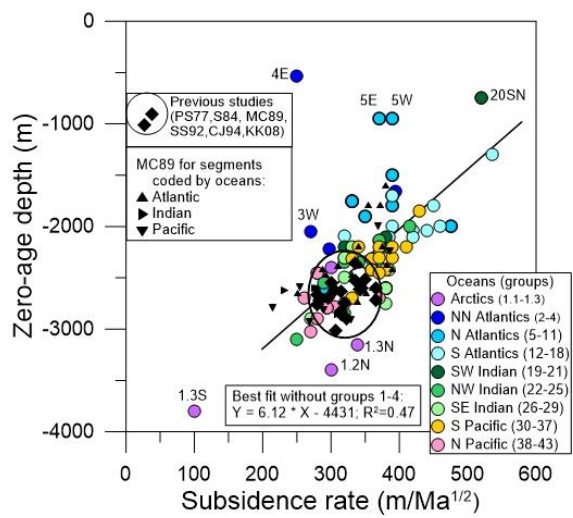
- (c) Sediments thickness based on previously published isopach maps, ocean drilling and seismic reflection profiles (*Divins, 2006*); in many places the database is constrained by the depth to the acoustic, not the “real”, basement and provides a minimum estimate. Red lines – mid-ocean ridges. Thin black lines – major transform faults, thin blue lines - rivers.
- (d) The effect of sediment correction (*Sykes, 1996*) which includes compaction of sediments with age (*Schroeder, 1984*). The effect is important along the Atlantic passive margins and at the Bengal Fan in the Indian Ocean with a large thickness of sediments (up to ca. 15 km).



**Supplementary Figure S2.**

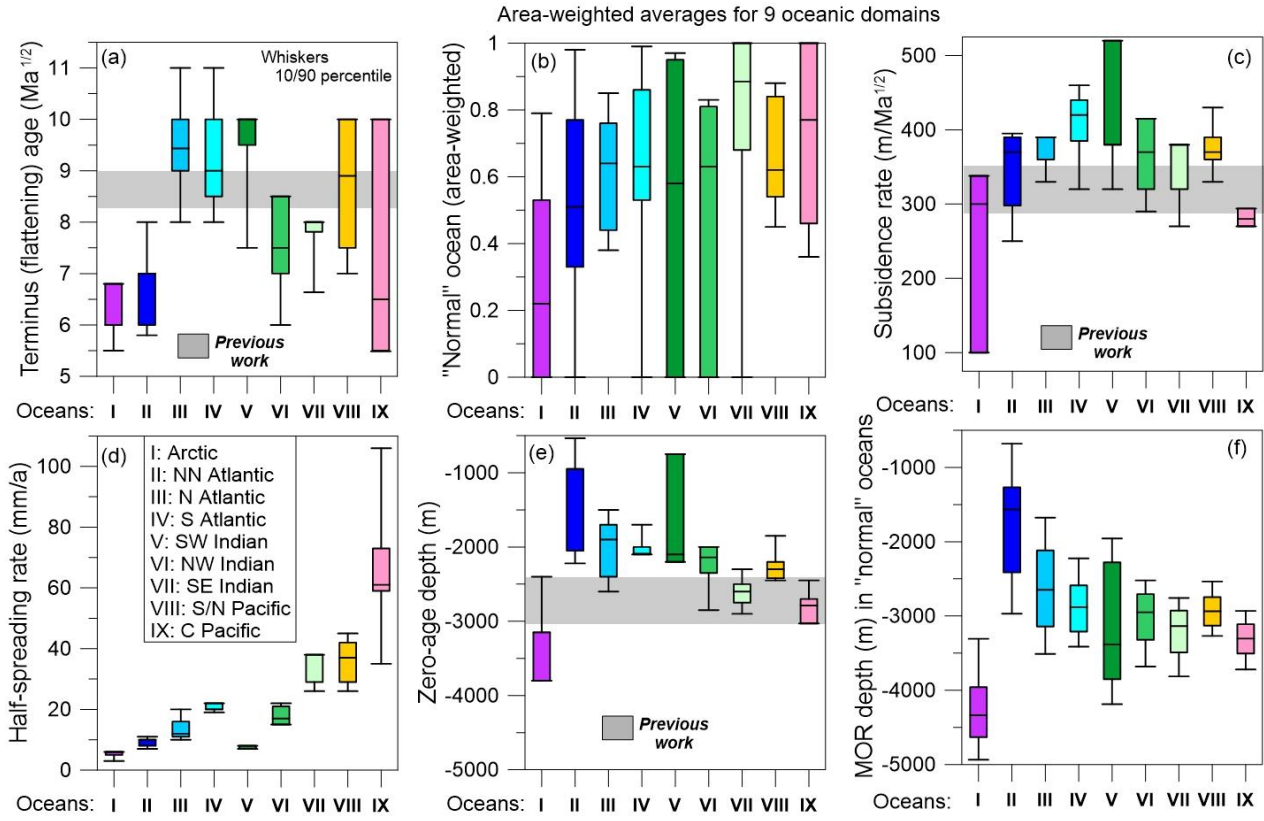
Examples illustrating the effect of sediment correction on bathymetry versus age evolution.

- (a) The effect of sediment compaction based on a standard correction (*Schroeder, 1984*).
- (b, c) Examples of sediment correction for two ocean segments (western North Atlantics and the Bengal Bay in the Indian Ocean) with present and paleo-spreadings (red dots – raw data for bathymetry, black dots – sediment-corrected values).



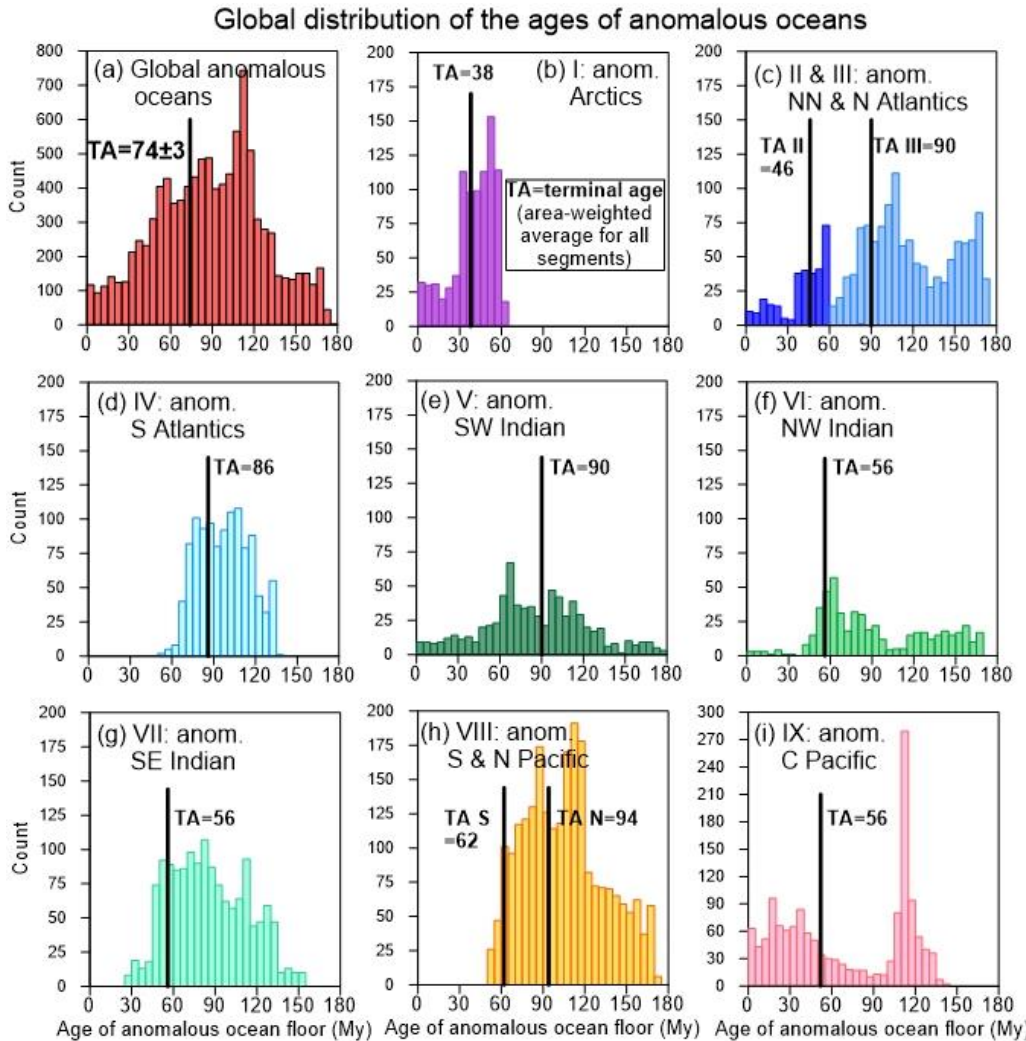
**Supplementary Figure S3.**

Comparison of subsidence rate and zero-age bathymetry (theoretical depth at mid-ocean ridges, Fig. 3a) estimated for 94 ocean segments (colored circles) in the present study and in previous studies (black symbols). Black triangles – 32 segments sorted by oceans (*Marty & Cazenave, 1989*); black rhombs – results by *Carlson & Johnson, 1994*; *Korenaga & Korenaga, 2008*; *Parsons and Sclater, 1977*; *Stein & Stein, 1992*; *Schroeder, 1984* (see Table S1 for details).



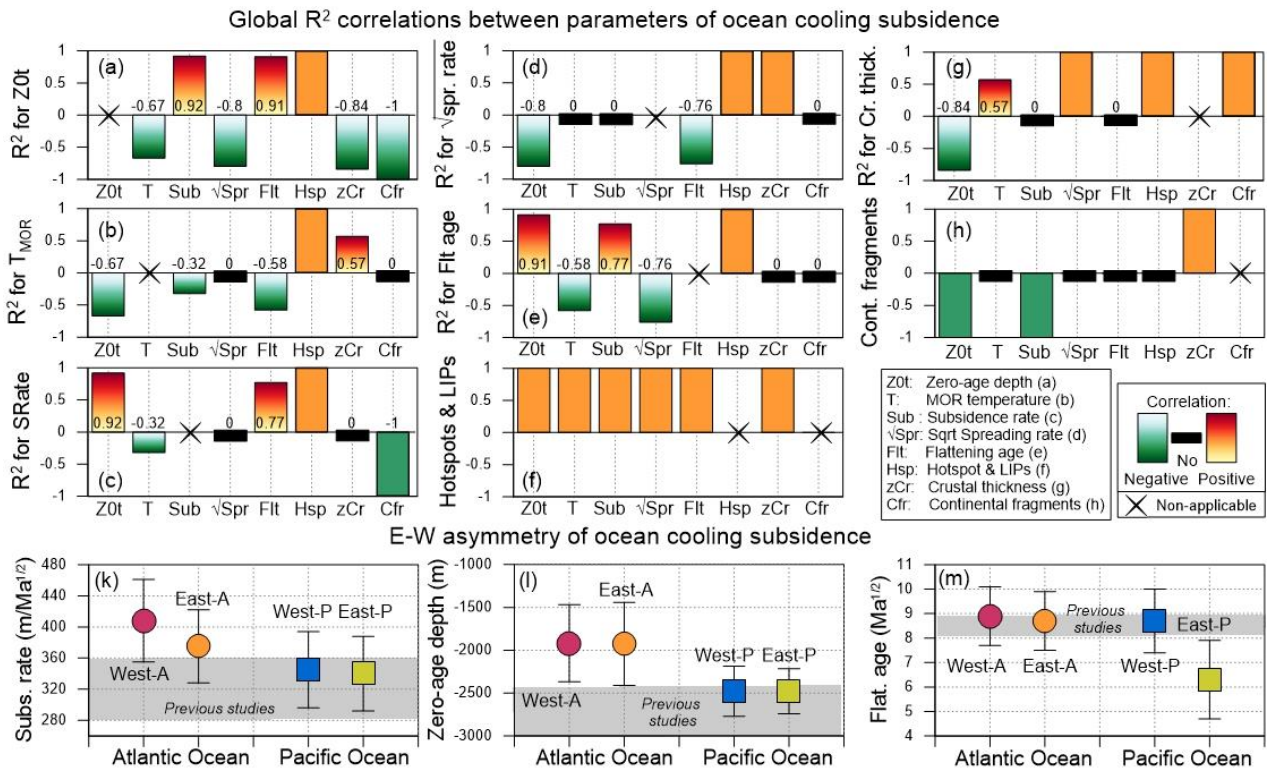
**Supplementary Figure S4.**

Area-weighted average values for oceanic segments determined in the present study. Boxes with whiskers statistics show average values (horizontal bars), total span of values (vertical lines), and the range for 90% of values (boxes color-coded by ocean domains). Ocean domains are numbered on the horizontal axes from I to IX. A large span of values implies highly heterogeneous cooling subsidence of the individual oceanic segments. Large deviations of the determined parameters from the previously reported "global" averages (gray shadings) imply that the latter are non-representative of any ocean and do not relate to any statistically significant portion of the ocean floor.



**Supplementary Figure S5.**

Age distribution of anomalous oceans impacted by hotspots with bathymetry deviation from square-root-of-age (averaged for 5 My bins). Black vertical lines – area-weighted terminus ages (TA, in My; error bars are <3 My) averaged for "good" segments in each oceanic domain (see Supplementary Table S2 for details). A global terminus ("flattening") age of  $74 \pm 3$  My (a) determined here is similar to the earlier published values, but it is significantly different in various segments and the ocean domains. In most ocean domains, significant parts of seafloor are younger than ocean-averaged terminus ages (left of the black lines). Several segments (3 in the Arctic Ocean, 2 in the Atlantic Ocean, 5 in the Indian Ocean, and 1 in the Pacific Ocean, see Methods) do not show a linear trend of bathymetry versus  $\text{sqrt}(\text{age})$  for any seafloor age and therefore have only anomalous ocean subsidence.



**Supplementary Figure S6.**

(a-h): Global correlation between pairs of the parameters related to isostatic cooling subsidence of "normal" oceans. Vertical axes show the level of correlation ( $-1 < R^2 < 1$ ), with positive correlations (when an increase in one parameter causes an increase in the other parameter) in warm colors and negative correlations in cold colors. Cases with the calculated  $R^2$ -values are shown in gradient colors ( $R^2$  values at the bars), solid colors are used when an overall correlation exists but cannot be quantified. Black bars mark uncorrelated pairs, crosses mark self-correlations.

(k-m): Statistical analysis of a possible east-west asymmetry of ocean cooling subsidence for the Atlantic and Pacific Oceans. The results do not imply an important role of west-drifting mantle flow in cooling subsidence of the Atlantic and Pacific Oceans.

**Supplementary Table S1. Previous analyses of oceanic lithosphere subsidence with reported  $\text{sqrt}(\text{age})$  cooling subsidence parameters**

Color highlights correspond to Fig. 2a.

Reference	Code (*shown in Fig. 1)	Ocean domain (**shown in Fig. S1)	Treatment of anomalous bathymetry	Comment on data analysis	Zero-age depth (m)	Subsi- dence rate (m/Ma <sup>1/2</sup> )	Flat- tening age (Ma)
Reference details			Data analysis		Reported values		
Global							
Carlson & Johnson, 1994	CJ94G*	Global**, based on local data for 42 DSDP/ODP drill sites	Excluded areas of anomalous bathymetry (around hot-spots, passive margins and trenches) and excluded zero-age drill sites	Test of PM and HSC models	-2600±20	345±3	73-80
Colin & Fleitout, 1990	CF90G*	Global, south of 53° N, on 1°x1° grid	Included (no cut-off) and excluded areas of anomalous bathymetry	Combined with geoid analysis • No cut-off: • Cut-off 300 m: • Cut-off 750 m:	-2762 -2722 -2607	280 366 342	N/A
Doin & Fleitout, 2000	DF00	Global, south of 60° N, on 5°x5° grid	Excluded areas of anomalous bathymetry	Combined with geoid analysis for 10 My age bins. Test of PM and CHABLIS models	N/A	240-440 for PM; 285±24 at 5 My	80-90
Kido & Seno, 1994	KS94	Global, on 1°x1° grid	Excluded dynamic topography with wavelength <5,000 km	Estimated dynamic topography from seismic tomography models	N/A	N/A	80

Korenaga & Korenaga, 2008	KK08G*	Global	Excluded areas of anomalously shallow (>1 km) bathymetry. Excluded regions with sediments >2 km	Statistical analysis. • Global data: • N Pacific & NW Atlantic:	-2630±150 -2760±130	315±26 317±21	70
Marty & Cazenave, 1989	MC89G*	Global**, S of 53° N, on 2°x2° grid	Excluded areas 1000 km away from hotspot swells & LIPs. Used old ocean age data	Split to 32 segments without following fracture zones: • Global: • Atlantic: • Indian: • S. Pacific:	Variable, -1510 to -3462  -2715 -2362±331 -2660±109 -2617±312	Variable 147 to 428  283 336±40 280±31 306±56	Variable 40-100 60-100 100 40-100
Smith & Sandwell 1997	SS97G*	Global	Excluded anomalous areas and oceans older 70 Ma, but kept thermal swells	Stochastic statistical analysis. Comparison of plate models.	-2950	320	55-70
<b>Atlantic &amp; Indian Oceans</b>							
Heestand & Crough, 1981	HC81A*	N Atlantic**, on 1°x1° grid, effectively between 15° N and 5° S	Excluded areas 1200-1800 km away from hotspot tracks. Old ocean age data.		-2700	295	60
Hayes, 1988	H88A* H88I*	S Atlantic & SE Indian, on 1°x1° grid	Excluded oceans older 100 Ma. No correction for sediment compaction	• S Atlantic: • SE Indian:	-2150 to -3000  -2600 to -3450	270 to 380  287 to 473	Variable
Crosby et al., 2006	C06A* C06I* CO6P*	Atlantic**, NW Indian & N Pacific** on 0.5°x0.5° grid	Excluded areas of anomalous bathymetry. Excluded areas with dynamic topography where gravity anomalies deviate from normal oceans	Test of PM & HCS models. Used 10 My age bins and gravity analysis • NE Atlantic: • SE Atlantic: • N Pacific:			
					-2527 -2444 -2821	336 347 315	80 80 70

N Pacific & N Atlantics							
Parsons & Sclater, 1977	PS77PA*	N Pacific & NW Atlantics**	Data along ship tracks and at DSDP sites. No filtering. Limited depth data for <10 Ma for N Pacific and <21 Ma for NW Atlantics. Used old age data	Based on Plate Model	-2500	-350	70
Stein & Stein, 1992	SS92PA*	N Pacific & NW Atlantics**	All data used. Limited depth data for <10 Ma oceans	Based on Plate Model. Split by 2 My age bins	-2600	365	70-80
Pacific Ocean							
Hillier & Watts, 2005	HW05P*	N Pacific**	Excluded areas of anomalous bathymetry	Account for lithosphere flexure, filtering of anomalous bathymetric features	-3010	307	85
Renkin & Sclater, 1988	RS88	N Pacific**	Excluded oceans older 80 Ma	Updated isochrons for W Pacific	N/A	N/A	80
Phipps Morgan & Smith, 1992	MS92P*	Pacific (no maps are included)	No information on data used	Theoretical models for mantle flow	-2544	300	70
Schroeder, 1984	S84P*	N & S Pacific**, on 2°x2° grid	Excluded areas 800 km away from hotspot tracks and trenches. Used old ocean age data. Data gaps 50° S to 10° N	<ul style="list-style-type: none"> <li>Linear fit is valid for ages &lt;160 Ma:</li> <li>Fit for ages &lt;80 Ma in case only trenches are excluded:</li> </ul>	-2890 -2846	314 298	160 80

## References to Table S1

- Carlson, R.L., & Johnson, H.P., 1994. On modeling the thermal evolution of the oceanic upper mantle: An assessment of the cooling plate model. *J. Geophys. Res.* 99, 3201–3214.
- Colin, P. & Fleitout, L., 1990. Topography of the ocean floor: thermal evolution of the lithosphere and interaction of deep mantle heterogeneities with the lithosphere. *Geophys. Res. Lett.*, 17, 1961–1964.
- Crosby, A., McKenzie, D., Sclater, J., 2006. The relations between depth, age and gravity in the oceans. *Geophysical Journal International*, 166, 553–573
- Doin, M.P. & Fleitout, L., 2000. Flattening of the oceanic topography and geoid: thermal versus dynamic origin, *Geophys. J. Int.*, 143, 582–594.
- Hayes D.E., 1988. Age-depth relationships and depth anomalies in the Southeast Indian Ocean and South Atlantic Ocean, *J. Geophys. Res.* 93, 2937-2954.
- Heestand, R.L. & Crough, S.T., 1981. The effect of hot spots on the oceanic age-depth relation. *J. Geophys. Res.*, 86, 6107-6114.
- Hillier, J.K., & Watts, A.B., 2005. Relationship between depth and age in the North Pacific ocean. *J. Geophys. Res.* 110, B02405.
- Kido, M., & Seno, T., 1994. Dynamic topography compared with residual depth anomalies in oceans and implications for age–depth curves. *Geophys. Res. Lett.* 21, 717–720.
- Korenaga, T. & Korenaga, J., 2008. Subsidence of normal oceanic lithosphere, apparent thermal expansivity, and seafloor flattening. *Earth and Planetary Science Letters*, 268, 41-51.
- Marty, J. C. & A. Cazenave, 1989. Regional variations in subsidence rate of oceanic plates: a global analysis. *Earth and Planetary Science Letters*, 94, 301-315
- Parsons, B., & Sclater, J. G., 1977. An analysis of variation of ocean-floor bathymetry and heat-flow with age. *J. Geophys. Res.* 85, 803-827.
- Phipps Morgan J., & Smith, W.H.F., 1992. Flattening of the sea-floor depth–age curve as a response to asthenospheric flow. *Nature* 359, 524– 527.
- Renkin, M.L., & Sclater, J.G., 1988. Depth and age in the North Pacific. *J. Geophys. Res.*, 93(B4): 2919-2935.
- Schroeder, W., 1984. The empirical age-depth relation and depth anomalies in the Pacific-ocean basin. *J. Geophys. Res.*, 89, 9873-9883.
- Smith, W.H., & Sandwell, D.T., 1997. Global sea floor topography from satellite altimetry and ship depth soundings. *Science* 277, 1956–1962.
- Stein, C.A. & Stein, S., 1992. A model for the global variation in oceanic depth and heat-flow with lithospheric age. *Nature*, 359, 123-129.

**Supplementary Table S2. Parameters of "normal" ocean subsidence for 94 ocean segments**

Rows – values determined for the individual ocean segments. Area-weighted averages (rows in gray) are determined for each ocean domain and presented as averages in all domain segments (all data) and only in "good" segments. Percentages for domain averages show areal portions of each domain with "normal" subsidence. In some "ugly" segments, the parameters cannot be determined due to data scatter. All values are rounded.

Central coord.	Segment number	Good, Bad, Ugly	Subsidence rate (m/Ma <sup>1/2</sup> )	Zero-age depth (m)	Terminus age (Ma <sup>1/2</sup> )	MOR depth (m) (<5 Ma)
<b>I: Arctic Ocean</b>						
108/86	1.1N	U	N/A	N/A	0	-4862±993
101/84	1.1S	U	N/A	N/A	0	-4897±1060
55/88	1.2N	U	300	-3400	5.5	-4007±213
56/85	1.2S	B	300	-2400	6	-4404
-2/85	1.3N	B	338	-3150	6	-4036±658
11/84	1.3S	U	100	-3800	6.8	-4161±488
<b>Weighted average (32% of area):</b>	<b>All data</b>		<b>242±105</b>	<b>-3264±502</b>	<b>6.2±0.4</b>	<b>-4200±674</b>
<b>II: Northern-most Atlantic Ocean</b>						
9/68	2E	U	N/A	N/A	0	-2763±256
6/78	2W	B	298	-2220	>8	-2983±340
5/72	3E	G	395	-1660	6	-2277±155
1/73	3W	B	270	-2050	6	-2605±297
-14/69	4E	U	250	-535	5.8	-1283±144
-17/70	4W	U	N/A	N/A		-992±664
-26/61	5E	B	370	-950	7	-1424±76
-30/62	5W	U	390	-950	7	-1006±450
<b>Weighted average (42% of area):</b>	<b>All data</b>		<b>344±54</b>	<b>-1307±584</b>	<b>6.8±0.7</b>	<b>-1853±852</b>
<b>Weighted average</b>	<b>Good only</b>		395	-1660	6	
<b>III: North Atlantic Ocean</b>						
-33/54	6E	G	330	-1750	8	-1939±493
-37/55	6W	G	330	-1750	9	-1676
-26/45	7E	B	390	-1500	10	-2147±324
-30/45	7W	G	390	-1700	11	-2347±809
-35/33	8E	B	350	-1900	10	-3176±1619
-39/35	8W	G	390	-1800	10	-2409
-44/23	9E	G	475	-2000	8	-3056±107
-48/23	9W	G	370	-2400	9	-3074±425
-39/10	10E	G	380	-2600	9	-2777±127
-44/10	10W	G	380	-2600	8.5	-3649±150
-28/2	11E	B	290	-2600	9	-3326±822
-32/1	11W	B	360	-2400	7.8	-2965±181
<b>Weighted average (60% of area):</b>	<b>All data</b>		<b>378±41</b>	<b>-1993±400</b>	<b>9.5±1.0</b>	<b>-2674±700</b>
<b>Weighted average</b>	<b>Good only</b>		<b>391±39</b>	<b>-2027±347</b>	<b>9.5±1.1</b>	
<b>IV: South Atlantic Ocean</b>						
-9/-4	12E	G	420	-2040	8	-3003±582

-14/-5	12W	G	440	-2040	8.5	-3202±526
-11/-17	13E	G	390	-2000	10	-2922±372
-17/-17	13W	G	460	-2000	8	-3050±530
-10/-28	14E	G	350	-2350	8.5	-3030±442
-16/-29	14W	G	385	-2100	8.5	-2978±493
-14/-42	15E	G	320	-2090	10	-2394±350
-19/-42	15W	G	420	-2100	11	-2568±198
-2/-50	16E	B	390	-1700	>7.42	-2748±669
-6/-52	16W	G	535	-1300	9	-2694±485
-16/-61	17S	G	450	-1800	9	-3464±513
19/-44	18E	U	N/A	N/A	0	N/A
10/-46	18W	U	N/A	N/A	0	N/A
<b>Weighted average (67% of area):</b>	<b>All data</b>		<b>407±54</b>	<b>-1995±234</b>	<b>9.3±1.1</b>	<b>-2888±472</b>
<b>Weighted average</b>	<b>Good only</b>		<b>408±55</b>	<b>-2013±231</b>	<b>9.4±1.1</b>	
<b>V: SW Indian Ocean</b>						
24/-51	19N	B	380	-2200	9.5	-3427±105
22/-54	19S	G	380	-2100	10	N/A
39/-42	20N	U	520	-750	9.5	N/A
38/-46	20S	U	520	-750	10	-2195±362
58/-13	21E	U	N/A	N/A	0	N/A
50/-36	21N	B	320	-2200	7.5	-3788±462
50/-39	21S	U	N/A	N/A	6.5	-3427±840
53/-17	21W	U	N/A	N/A	0	N/A
<b>Weighted average (51% of area):</b>	<b>All data</b>		<b>424±75</b>	<b>-1636±677</b>	<b>9.5±0.8</b>	<b>-3146±722</b>
<b>Weighted average</b>	<b>Good only</b>		380	-2100	10	
<b>VI: NW Indian Ocean</b>						
58/-13	22.1E	U	N/A	N/A	5	N/A
61/8	22E	G	320	-2850	7.5	N/A
42/-5	22N	U	N/A	N/A	0	N/A
47/-4	22S	U	N/A	N/A	0	N/A
59/6	22W	U	250	-3100	7	-3609±137
68/0	23E	G	340	-2350	7	-2891±64
66/-2	23W	G	290	-2550	7.5	-2910±691
68/-12	24E	G	370	-2140	6	-2897±275
64/-14	24W	G	320	-2350	6	-3063±523
70/-21	25E	G	415	-2000	8.5	-2946±460
67/-22	25W	G	370	-2140	7.5	-2900±617
<b>Weighted average (57% of area):</b>	<b>All data</b>		<b>355±50</b>	<b>-2284±320</b>	<b>7.5±0.8</b>	<b>-3021±436</b>
<b>Weighted average</b>	<b>Good only</b>		<b>361±44</b>	<b>-2240±264</b>	<b>7.5±0.9</b>	
<b>VII: SE Indian Ocean</b>						
95/-11	26E	U	N/A	N/A	0	N/A
77/-29	26N	G	320	-2500	>6.63	-2837±224
74/-32	26S	B	270	-2900	8	-3005±477
90/-6	26W	U	N/A	N/A	0	N/A
81/-40	27N	G	320	-2300	5.5	-2740±270
79/-43	27S	G	320	-2300	5	-2768±167
114/-48	28N	G	380	-2750	8	-3154±377

114/-52	28S	G	380	-2600	8	-3220±317
151/-57	29N	G	385	-2420	>7.48	-2907±197
150/-61	29S	G	330	-2200	>7.81	-2653±395
<b>Weighted average (62% of area):</b>	<b>All data</b>		<b>352±42</b>	<b>-2623±192</b>	<b>7.6±0.8</b>	<b>-3211±437</b>
<b>Weighted average</b>	<b>Good only</b>		<b>367±25</b>	<b>-2572±163</b>	<b>7.6±0.9</b>	
<b>VIIIIs: South Pacific Ocean</b>						
-170/-66	30E	G	340	-2200	7	-2717±190
-173/-63	30W	G	370	-2200	8.5	-2675±239
-148/-60	31E	G	360	-2320	7.5	-2828±92
-153/-59	31W	G	367	-2290	8.9	-2617±159
-137/-55	32E	G	410	-2200	7.5	-2755±345
-141/-55	32W	G	307	-2390	9.2	-2754±663
-116/-53	33E	G	390	-2300	7	-2901±227
-120/-53	33W	G	370	-2300	8	-2828±286
-109/-43	34E	G	380	-2420	>6.71	-2846±202
-113/-43	34W	B	390	-2200	7.5	-2763±177
<b>Weighted average (70% of area):</b>	<b>All data</b>		<b>370±26</b>	<b>-2271±64</b>	<b>7.8±0.8</b>	<b>-2918±277</b>
<b>Weighted average</b>	<b>Good only</b>		<b>366±26</b>	<b>-2288±60</b>	<b>7.9±0.8</b>	
<b>VIIIIn: North Pacific Ocean</b>						
-108/23	39W	G	360	-2420	9	-2831±355
-116/30	40W	G	360	-2420	9	N/A
-122/36	41W	G	330	-2700	10	N/A
-125/40	42W	G	370	-2450	10	-2767±528
-131/49	43W	B	430	-1850	10	-2556±284
<b>Weighted average (62% of area):</b>	<b>All data</b>		<b>376±36</b>	<b>-2314±308</b>	<b>9.7±0.5</b>	<b>-2937±420</b>
<b>Weighted average</b>	<b>Good only</b>		<b>355±15</b>	<b>-2498±117</b>	<b>9.5±0.5</b>	
<b>VIII: South &amp; North Pacific Ocean</b>						
<b>Weighted average</b>	<b>All data</b>		<b>370±28</b>	<b>-2308±183</b>	<b>8.4±1.1</b>	<b>-2920±295</b>
<b>IX: Central Pacific Ocean</b>						
-110/-29	35E	B	280	-2450	5.5	-2955±217
-114/-29	35W	G	280	-2450	>7.07	-2802±327
-111/-16	36E	U	320	-2750	3.5	-3138±220
-115/-16	36W	B	260	-2700	6	-3030±214
-100/-5	37E	B	280	-2900	>5.48	-3313±192
-108/-4	37W	B	370	-2700	6.5	-3223±195
-101/9	38E	B	305	-2780	>4.25	-3141±259
-106/9	38W	G	270	-3030	10	-3333±261
-87/3	44EW	U	N/A	N/A	0	-2825±412
-86/-40	45N	G	294	-2788	>6.16	-3110±213
-86/-44	45S	G	294	-2788	>7.0	-3278±196
<b>Weighted average (71% of area):</b>	<b>All data</b>		<b>280±14</b>	<b>-2806±205</b>	<b>7.2±2.0</b>	<b>-3302±323</b>
<b>Weighted average</b>	<b>Good only</b>		<b>278±11</b>	<b>-2871±2087</b>	<b>8.6±1.6</b>	
<b>Global</b>						
<b>Weighted average (60% of area):</b>	<b>All data, without 1-4</b>		<b>357±59</b>	<b>-2319±481</b>	<b>8.3±1.6</b>	<b>-3022±639</b>
<b>(42% of area):</b>	<b>Good only</b>		<b>361±53</b>	<b>-2379±354</b>	<b>8.6±1.4</b>	